WILEY InterScience® DISCOVER SOMETHING GREAT

The effect of yield damage on the viscoelastic properties of cortical bone tissue as measured by dynamic mechanical analysis

Yener N. Yeni,[1] Richard R. Shaffer,[1] Kevin C. Baker,[1] X. Neil Dong,[1] Michele J. Grimm,[2] Clifford M. Les,[1] David P. Fyhrie[3]

[1]*Bone and Joint Center, Henry Ford Hospital, 2799 West Grand Boulevard, Detroit, Michigan 48202*
[2]*Department of Biomedical Engineering, Wayne State University, Detroit, Michigan*
[3]*Department of Orthopaedic Surgery, University of California, Davis, Sacramento, California*

Received 8 September 2006; revised 20 October 2006; accepted 6 November 2006
Published online 12 February 2007 in Wiley InterScience (www.interscience.wiley.com). DOI: 10.1002/jbm.a.31169

Abstract: We have previously shown, using Dynamic Mechanical Analysis (DMA), that the presence of a defect in cortical bone tissue affects the apparent viscoelastic properties of that bone. However, mechanically induced damage is more complex than a machined defect making it difficult to predict its effect on bone viscoelasticity. We performed DMA measurements before and after introduction of yield damage into cortical bone beams from sheep radii. The specimens were placed in a DMA machine and baseline measurements of storage modulus (E1) and loss factor (tan δ) were performed using a 3-point bending configuration for a frequency range of 1–10 Hz. Measurements were done in all four bending directions (cranial, caudal, medial, and lateral) in random order. After subjecting the specimens to monotonic yield damage in a servohydraulic testing machine with the load applied to the cranial surface, oscillatory tests were repeated. To supplement results from the current experiment, additional analyses were performed on data from experiments where bone was either cut or fatigue-loaded between viscoelasticity measurements. Introduction of mechanical damage increased tan δ and frequency sensitivity of E1, consistent with the assertion that increased energy dissipation in damaged bone might contribute to its increased resistance to fatigue and fracture. © 2007 Wiley Periodicals, Inc. J Biomed Mater Res 82A: 530–537, 2007

Key words: cortical bone; dynamic mechanical analysis; viscoelastic properties; yield damage; energy dissipation

INTRODUCTION

Naturally occurring flaws in the form of microdamage exist in human bone tissue and tend to increase with aging.[1–4] Bone microdamage as a result of fatiguing activities has been implicated in a number of conditions including loosening of joint prostheses,[5] subchondral bone stiffening and osteoarthrosis,[6,7] stress fractures,[8] and an increase in bone fragility and osteoporotic fractures.[9–14] Despite its potentially harmful effects on the mechanical integrity of bone tissue, however, the exact nature of the interaction between microdamage and mechanical behavior of bone is not well-understood. It is generally believed that, left unrepaired, the presence of these microcracks predisposes the tissue for failure during subsequent loading by reducing its ability to withstand load and resistance to fatigue and fracture.[15–22] On the other hand, it has also been reported that longer fatigue life was associated with higher rather than lower initial crack density when the effect of modulus variability was controlled.[23]

We believe that an increase in the ability of bone tissue to dissipate energy through viscoelastic means during damage accumulation may enhance its fatigue and fracture resistance since less of the energy will be available for creation of new crack surfaces. We have demonstrated in our previous work that the presence of a flaw in bone tissue can be detected using frequency analysis of dynamic properties from nondestructive oscillatory tests.[24] Although the use of a machined flaw provided information on the effect of a large (on the order of 1 mm) and highly concentrated defect with known geometries on the viscoelastic behavior of bone, it is not clear whether this can be extrapolated to mechanically induced

Correspondence to: Y. N. Yeni, Ph.D., Head, Section of Biomechanics, Bone and Joint Center, Henry Ford Hospital, 2799 West Grand Boulevard, Detroit, Michigan, 48202, USA; e-mail: yeni@bjc.hfh.edu

Contract grant sponsors: National Institutes of Health; contract grant numbers: AR40776, AR47434, AR049343

© 2007 Wiley Periodicals, Inc.

damage. In this study, we examined the effect of minimal mechanical damage (created by loading bone tissue just beyond yield) on the subsequent viscoelastic behavior of cortical bone tissue.

In order to gain additional insight into the effect of damage on the damping ability of bone, we revisited our previous work where damage was introduced by cutting the bone specimens.[24] This allowed us to recalculate the parameters of that study in a way consistent with the current design and to perform a more comprehensive statistical analysis. We also revisit an experiment where data were available from bone specimens that were damaged using fatigue loading and subjected to ultrasound measurements before and after fatigue damage.[15] In that experiment, ultrasound measurements were performed on a group of specimens with aims not relevant to the current study. Our overall hypothesis was that damage would affect the viscoelastic properties of cortical bone consistent with our assertion that damaged bone is more energy-dissipative. The revisited experiments were expected to provide more insight into the nature of the interaction between damage and energy dissipation properties.

METHODS

Left radii from seven sheep were used (eight-year-old Warhill sheep). A 65 mm bone segment was cut out of each radius such that 25 mm proximal and 40 mm distal regions with respect to the center were included. The bone segment was clamped from the distal end and cortical bone beams ($2 \times 2 \times 19$ mm^3) were machined from the proximal piece using the Exakt cutting system (Exakt Technologies, Oklahoma City, OK) resulting in middiaphyseal specimens with the long axis of the beam being aligned with the long axis of the bone. One beam per bone was randomly selected from the cranial cortex of each radius. The experiment involved dynamic mechanical analysis (DMA) of bone beams before and after the introduction of yield damage (Fig. 1).

The specimens were placed in a dynamic mechanical analyzer (DMA 7e, PerkinElmer, Norwalk, CT) and baseline viscoelastic measurements were performed in 0.9% saline solution at 37°C from oscillatory tests using a 3-point bending configuration (15 mm span length).[25] A calcium buffer in the saline solution, which is recommended for long-term experiments,[26] was not used in this experiment. However, it is unlikely that the leaching of calcium would significantly affect the results as the total amount of time spent for measurements was less than 45 min. We have also verified in a separate study that there are no significant differences in cortical bone tissue properties between two subsequent measurements in our DMA system.[27] A 550 mN static and 500 mN dynamic load waveform was used as the oscillatory input (Fig. 1), scanning a frequency range of 1–10 Hz (in 0.2 Hz increments).[24,28] Storage modulus, E1 (for dynamic tests, equivalent to Young's modulus) and loss factor, tan δ (an indication of the amount of energy dissipated by viscous mechanisms relative to energy stored in the elastic component) were measured for each of the cranio-caudal (cranial bending: load applied to the cranial surface), caudal-cranial (caudal bending: load applied to the caudal surface), medio-lateral (medial bending: load applied to the medial surface) and latero-medial (lateral bending: load applied to the lateral surface) bending directions.

Specimens were then subjected to yield damage under 3-point bending using a servohydraulic testing machine (Instron 8501M, Canton, MA). The damaging load was applied to the cranial surface of specimens. Displacement rates corresponding to a strain rate of 0.001 s^{-1} were used. Beam equations were used for calculations of strain and strain rate.[29] Yield damage point was reached by application of successive monotonic loading with 5N increments starting from 25N (unloaded between increments). Loading was discontinued when the stress-strain curve passed the point of intersection with the 95% secant modulus line [Fig. 1(d)]. Specimens were kept wet with 0.9% saline solution during testing. After the specimens were damaged, oscillatory tests were repeated in the DMA machine. Specimens and loading directions were tested in a random order in order to avoid a potential systematic effect caused by sequential testing of loading directions.

Because storage modulus and tan δ exhibit a strong power-law and a linear relationship with frequency ($E1 = Af^B$ and $\tan\delta = -C f + D$; f = frequency), respectively, the fit parameters A, B, C, and D were examined as the viscoelastic parameters for each measurements for each specimen. Two way repeated measures ANOVA was used with bending direction (cranial, caudal, lateral, medial) and test (predamage, postdamage) as factors. When significance was detected, Fisher's LSD test was used to isolate group differences.

The results of a previous experiment[24] were reanalyzed as described above in order to compare with the current results. In that experiment, all test parameters were the same as the current, except that the specimens were resubjected to a DMA test after cutting a defect at the center of beams instead of introducing damage using mechanical loading. Specimens in the defect experiment were initially stiffer (Coefficient A) ($p = 0.028$) and had lower initial tan δ (intercept D) ($p = 0.026$) than those in the yield experiment. After examination of the effect of bending directions and damage for each experiment, the comparison of the yield and the defect experiments were done using a mixed model with the damage mode (yield vs. cut defect) as a factor, frequency (1 Hz vs. 10 Hz) as a repeated factor and the percent change in tan δ under cranial bending as the outcome variable.

In order to investigate whether mechanical damage causes changes in tan δ at high frequencies, we revisited a previously conducted experiment where the effect of fatigue damage on fracture toughness was investigated.[15] A subset of the specimens in that experiment was subjected to ultrasound tests before and after fatigue loading but those data were not analyzed in the manner reported here. A complete set of data was available from seven specimens of a previous study. Rectangular beam specimens ($4 \times 4 \times 48$ mm^3) were machined from bovine tibiae using a low-speed diamond saw (Model 660, South Bay

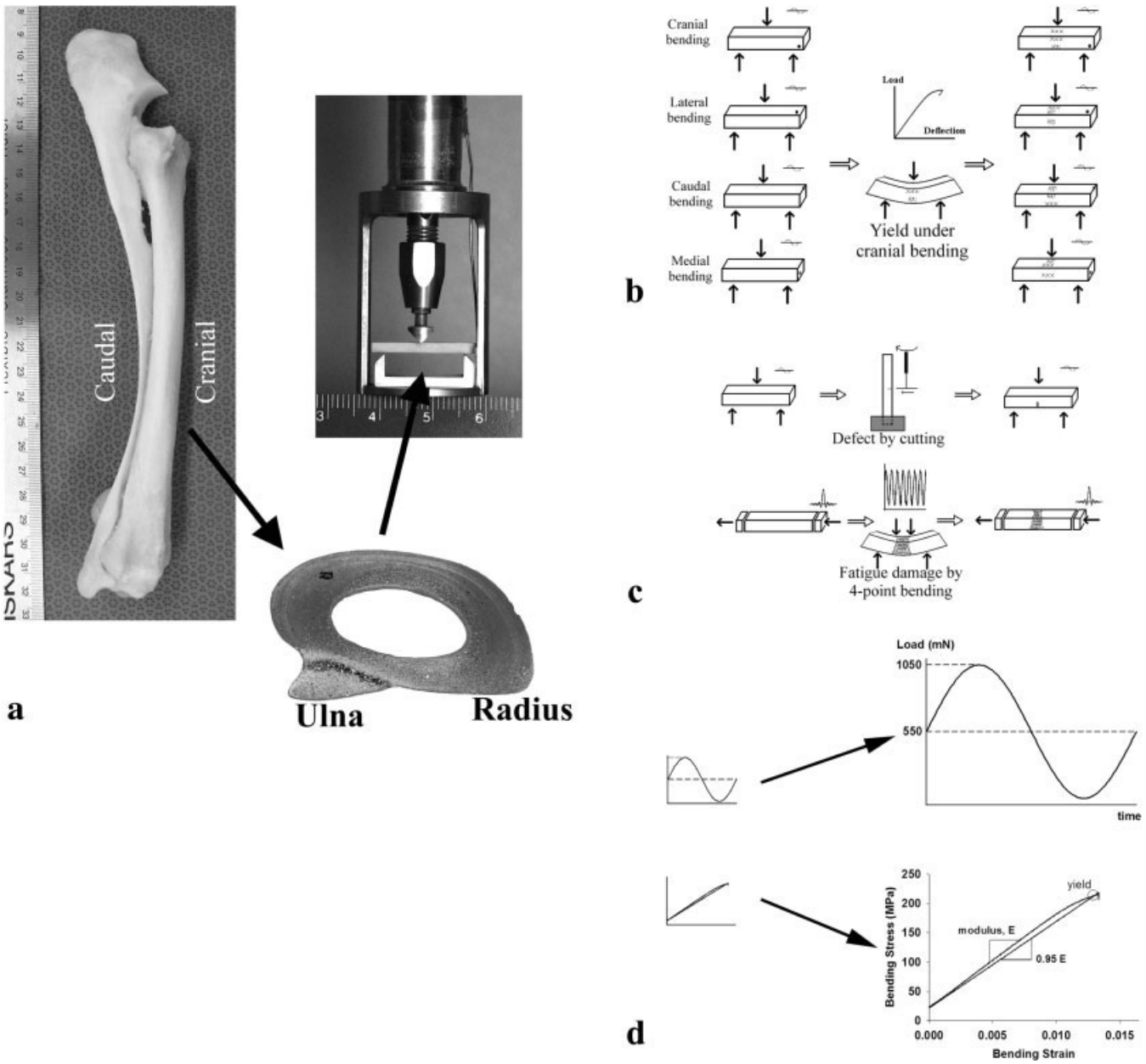

Figure 1. (a) Flow of specimen preparation from sheep radii. (b) Specimen flow during the experiment. Cortical bone beams were subjected to three-point bending DMA analysis in four orientations. The black point marks the proximal end and the lateral cortex of the bone beams and can be used as a reference for bending directions. The beams were vibrated once in the craniocaudal (load applied to the cranial surface), once in the caudocranial (load applied to the caudal surface), once in the lateromedial (load applied to the lateral surface), and once in the mediolateral (load applied to the medial surface) direction. The specimens then were subjected to yield-damage in three-point craniocaudal bending. DMA measurements were repeated in all four bending directions. (c) The configuration of the revisited experiments to illustrate the differences from the current experiment. A defect was introduced by cutting a notch between DMA measurements (top) or the specimen was subjected to 4-point bending fatigue damage between transmitted ultrasound measurements (bottom). (d) The details of the DMA waveform (top) and determination of yield point (bottom).

Technology, Temple City, CA). The long axes of the beams were aligned with the long axis of bone. Using a four point bending fatigue setup, the specimens were fatigue damaged to different levels of stiffness loss at 2 Hz under load control corresponding to an initial strain of 5000 με.[30] The specimens were subjected to ultrasonic tests before and after fatigue loading. Ultrasonic velocity and amplitude measurements were performed using 1 MHz contact type pressure-wave transducers (V103-RB, Panametrics, MA), a pulse generator/receiver, and an oscilloscope in through-transmission mode. Water was used as the coupling medium between the bone and the pressure-wave transducer. Ultrasound measurements were made in the long direction of beam. Time-to-travel and amplitude

information were recorded from the oscilloscope reading along with a reference signal from the pulse generator. These measurements allow for calculation of tan δ using the relationships[31]: $\alpha = (\omega/c) \tan(\delta/2)$ and $\alpha = \ln(A_1/A_2)/(L_1-L_2)$ where α is attenuation, A_1 and A_2 are magnitudes of the wave transmitted through materials of length L_1 and L_2 but of identical construct, ω is the angular frequency and c is the speed of the transmitted wave. The input signal (for $L_1 = 0$) from the pulse generator was used as a reference eliminating potential errors from the variability of construct between two specimens that need to be identical in construct. With L_1, L_2, and ω known, A_1, A_2, and c were measured. From these tan δ were calculated. The formula that relates attenuation to tan δ should be considered approximate (and used on a comparative basis) as it does not have explicit terms that represent microstructure such as pores. A paired t-test was used to compare prefatigue and postfatigue tan δ measurements. Regression analysis was used to examine the relationship between changes in tan δ and stiffness due to fatigue damage.

RESULTS

For the beams loaded to yield in the current study, the frequency-dependence of tan δ (C; absolute value of the slope of the tan δ-frequency regression for each measurement) significantly decreased after yield-load ($p < 0.006$) (Table I). The effect of bending mode on C or the interaction between bending mode and pre/postyield measurements were not significant ($p = 0.159$ and $p = 0.718$, respectively) (Fig. 2).

The effect of bending mode or pre- versus postyield measurements on the intercept D of tan δ-frequency regressions were not significant ($p = 0.771$ and $p = 0.919$, respectively) (Table I). The interaction between bending mode and pre/postyield measurements was not significant, either ($p = 0.150$).

The effect of bending mode or pre- versus postyield measurements on the coefficient A of storage modulus-frequency regressions were not significant ($p = 0.550$ and $p = 0.161$, respectively) (Table I). The interaction between bending mode and pre/postyield measurements was not significant, either ($p = 0.104$).

The exponent B of the storage modulus-frequency relationship significantly increased after yield-load ($p = 0.038$) (Table I). The effect of bending mode on B or the interaction between bending mode and pre/post-yield measurements were not significant ($p = 0.980$ and $p = 0.443$, respectively).

For the beams with a machined defect (reanalysis of data from Yeni et al.[24]), the effect of bending mode or pre- versus postdefect measurements on the slope C of tan δ-frequency regressions were not significant ($p = 0.949$ and $p = 0.231$, respectively) (Table I). The interaction between bending mode and pre/postyield measurements was not significant, either ($p = 0.756$).

The intercept D of tan δ-frequency regressions was significantly greater for cranial bending than for medial bending ($p = 0.020$) and increased after machining the defect ($p = 0.004$) (Table I). The interaction between bending mode and pre/postdefect measurements was marginally significant ($p = 0.074$) suggesting that the effect of machined defect depends on the bending direction as well.

Coefficient A of storage modulus-frequency regressions was larger in medial bending than cranial bending ($p = 0.018$) and decreased after machining the defect ($p = 0.013$) (Table I). The interaction between bending mode and pre/postdefect measurements was also significant ($p = 0.047$). Post-hoc analysis indicated that the greater reduction was for cranial bending and that the difference in medial and cranial bending was due to the defect ($p = 0.002$).

The exponent B of the storage modulus-frequency relationship significantly decreased after machining a defect ($p = 0.036$) (Table I). The effect of bending mode on B or the interaction between bending mode and pre/postyield measurements were not significant ($p = 0.153$ and $p = 0.199$, respectively).

The increase in tan δ due to a machined defect was greater than that due to loading to yield ($p = 0.016$) and was also greater for 10 Hz than for 1 Hz ($p = 0.005$; RMANOVA). The dependence of increase in tan δ with frequency was not affected by the type of damage (yield-load vs. machined-defect) (Fig. 3).

For the beams fatigue tested and measured using ultrasound, postfatigue increase in tan δ correlated with the increase in stiffness loss indicating that viscoelastic dissipation increases as mechanical damage increases under bending-fatigue (Fig. 4). On the average, postfatigue tan δ (0.0579 ± 0.0122) was greater than prefatigue tan δ (0.0570 ± 0.0142), however, this was not significant ($p = 0.483$; paired t-test) owing to one specimen with decreased tan δ after fatigue ($p = 0.056$ if it is excluded).

DISCUSSION

Viscoelastic properties of cortical bone tissue were examined before and after loading to yield. New data and data from previous experiments were analyzed together to gain additional insight into the role of mechanical damage on viscoelastic property changes in bone tissue. We observed that mechanical damage causes significant changes in the viscoelastic properties of cortical tissue.

The morphology of the damage was not examined in the current experiments. Mechanical property degradation is the direct manifestation of damage,

TABLE I
Coefficients C, D, A, and B of Fits "tanδ = −Cf + D" and "E1 (GPa) = Af^{B}"

	Preyield	Postyield	Predefect	Postdefect
Slope C[a]				
Caudal	0.00379 ± 0.00090	0.00289 ± 0.00089		
Cranial	0.00356 ± 0.00106	0.00284 ± 0.00090	0.00380 ± 0.00066	0.00403 ± 0.00053
Lateral	0.00386 ± 0.00096	0.00335 ± 0.00037		
Medial	0.00385 ± 0.00087	0.00337 ± 0.00099	0.00372 ± 0.00076	0.00415 ± 0.00064
Intercept D[b]				
Caudal	0.0843 ± 0.0188	0.0773 ± 0.0092		
Cranial[c]	0.0786 ± 0.0084	0.0822 ± 0.0059	0.0707 ± 0.0033	0.1108 ± 0.0256
Lateral	0.0845 ± 0.0130	0.0826 ± 0.0103		
Medial	0.0793 ± 0.0154	0.0835 ± 0.0133	0.0634 ± 0.0081	0.0751 ± 0.0067
Coefficient A[b]				
Caudal	12.0 ± 2.1	11.9 ± 2.2		
Cranial[c]	11.8 ± 3.1	11.9 ± 2.8	14.9 ± 2.8	9.5 ± 2.8
Lateral	11.2 ± 1.2	11.0 ± 1.1		
Medial	11.9 ± 1.3	11.0 ± 1.1	15.2 ± 2.6	13.0 ± 2.1
Exponent B[ab]				
Caudal	0.0387 ± 0.0114	0.0395 ± 0.0095		
Cranial	0.0366 ± 0.0102	0.0405 ± 0.0089	0.0367 ± 0.0035	0.0262 ± 0.0106
Lateral	0.0378 ± 0.0076	0.0412 ± 0.0070		
Medial	0.0385 ± 0.0101	0.0407 ± 0.0057	0.0284 ± 0.0034	0.0259 ± 0.0059

[a]Significant difference between pre- and postyield measurement.
[b]Significant difference between pre- and postdefect measurement.
[c]Significant difference between cranial and medial bending in the machined-defect experiment.

however, a full explanation of the degradation is not possible using only morphological measures of damage.[17,32,33] In previous work by Jepsen and co-workers, the increase in damage (quantified as the density of histologically observable microcracks) did not explain changes in bone viscoelasticity. They concluded that measures of damage other than crack density are necessary to explain tissue level viscoelastic property changes.[34] We used modulus change criteria as a direct indication of damage in our specimens. Stiffness loss and damage accumulation due to fatigue loading in cortical bone is well-documented.[18,20,30,32] Therefore, stiffness loss was used as an indication of fatigue damage in the fatigue experiment. The use of change in secant modulus to describe damage or initiation of failure is a standard application.[35–37] In the current study, we used 5% change in secant stiffness to define the yield point which was considered as the minimum described damage in our bending experiment.

Damaged cortical bone is more viscoelastic as shown by increases in dissipation (tan δ parameters). Viscoelasticity observed at the macro-scale is due to an unknown number of molecular level energy dissipation mechanisms and is affected by damage at the molecular level. The energy dissipation mechanism may include: the opening and closing of crack faces, sliding at damaged interfaces, shifting of defects in

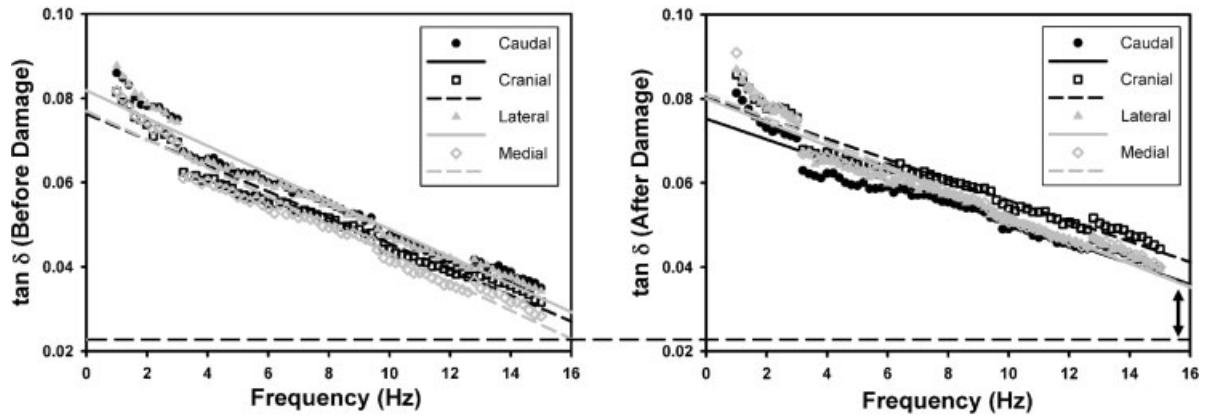

Figure 2. The similarity of the intercepts and the significant decrease in the (absolute) slopes of tan δ-frequency regressions after yield indicates an increase in post-yield tan δ for higher frequencies tested. For illustration purposes, regression lines are fitted to the data averaged over seven specimens for each bending direction.

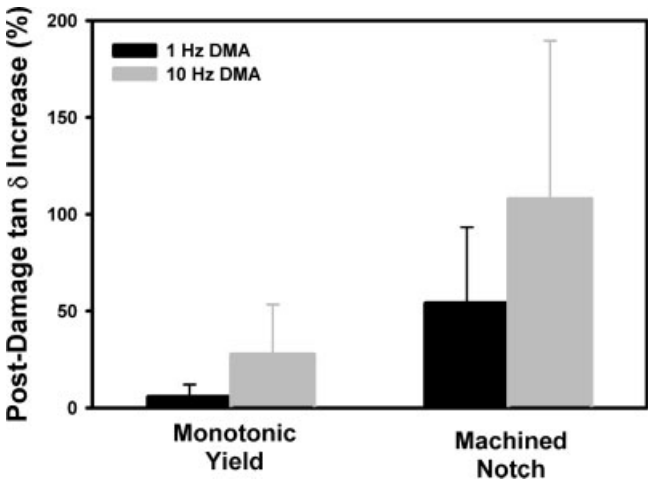

Figure 3. The increase in tan δ with type of damage and frequency. Error bars indicate standard deviation. See text for statistical comparison.

the mineral phase, rupturing of molecules in the organic phase (breaking cross-links or collagen unwinding), change in the amount of fluid flow and strain rate amplification at the crack tip. Viscoelastic frequency scanning is a common approach for getting insight into the active energy dissipation mechanisms in composites. The power of the method results from the fact that each energy dissipation-mechanism activates in a predictable range of frequencies[38] and is detectable in the data even if the exact nature of the mechanism is not known. Our DMA results (within 1–10 Hz) and results of creep/relaxation tests from others indicate that mechanical damage affects the low-frequency mechanisms. The observed correspondence between an increase in tan δ as measured from a high-frequency method and an increase in stiffness loss during fatigue suggests that mechanical damage also affects activation of high-frequency energy dissipation mechanisms in bone tissue. The introduction of damage through 3-point bending in low-frequency experiments and through 4-point bending in high-frequency experiments makes it difficult to sort out the role of shear damage vs tensile or compressive damage, however, this does not detract from the generality of the results.

In the notch-cutting experiment, a large structural defect with a known size and geometry was introduced without causing true material changes at the microscale. In this case, the reduction in the power-exponent of modulus-frequency relationship can be explained by strain rate amplification at the notch tip. Because the effective loading rate is larger than the rate in an undamaged bone at the same loading, the storage modulus increased due to the strain rate effect and was evaluated within a range in which it is less frequency-sensitive. In the yield-load experiment, the power-exponent increased together with increasing tan δ consistent with a change in the tissue that was not caused by a change in beam geometry.

It has been shown that mechanical damage reduces crack initiation fracture toughness in bone (indicative of a reduction in the threshold energy for initiation of a crack).[15] On the other hand, the increased tan δ in damaged bone indicates that it would be more difficult to propagate a crack as more of the energy in a loading cycle can be dissipated by means other than crack growth in the damaged bone. This is consistent with observations that bone exhibits a rising R-curve behavior.[39–41] We hypothesize that increased viscoelasticity by mechanical damage may serve as a toughening mechanism in bone. A number of concurrent mechanisms such as microcracking and bridging[41,42] may be involved in the rising R-curve behavior of bone. The toughening by increased viscoelastic energy dissipation with damage is distinct in that it can explain the increase of bone toughness with increasing strain-rate despite occurrence of fewer microcracks.

The changes in tan δ and power exponent observed in the yield-experiment were without notable changes in the magnitude of storage modulus for the yield-load experiment. This could mean that viscoelastic properties are more sensitive to incipient damage than elastic properties in bone tissue. Changes in storage modulus, being analogous to Young's modulus for monotonic loading, would be indicative of changes in strength due to the strong correlation between modulus and strength of cortical bone tissue with or without damage.[15,43,44] The earlier change in tan δ and rate-dependence of the tissue with damage suggests that there are changes in the postyield properties of bone due to small amounts of mechanical overload before loss of stiffness and strength is observed.

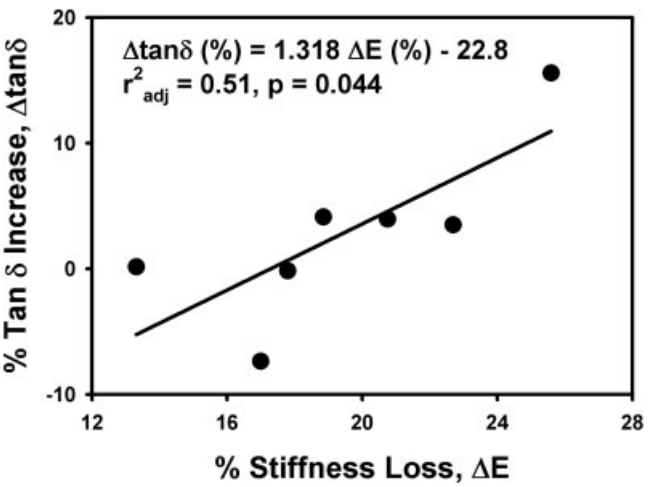

Figure 4. Increase in tan δ (from ultrasound measurements) with increase in stiffness loss post-fatigue indicating that viscoelastic dissipation increases as mechanical damage increases under bending-fatigue.

Energy dissipation mechanisms activated by higher frequencies as in this study are usually associated with size-scales corresponding to ultra- to molecular structures rather than microstructure. Analyses of fracture surfaces show that the failure of mineralized fibrils is a common element in the fracture of different bone tissue types.[45–47] Delamination of the fibrillar structure through the failure of interfibrillar noncollagenous proteins is the likely failure mechanism for mineralized fibrils. Breaking and reforming of bonds within or between interfibrillar noncollagenous proteins, or between noncollagenous proteins and the mineral surface has been suggested as a toughening mechanism at this scale.[48–50] Although mechanical damage may ultimately influence the effectiveness of these "sacrificial" bonds, the direct effect must be of more permanent nature as it could be observed at a much longer time scale than that is relevant to breaking and reforming the sacrificial bonds. We believe that incipient mechanical damage involves permanent breakage of some of these interfibrillar bridges. It is not clear which noncollagenous proteins provide the interfibrillar bridges in bone, however, it is thought that Ca^{++}-binding species are involved[48,49,51] Based on the current observations, identification of damage mechanisms at the collagen/mineral level that affect energy dissipation should provide further insight into fracture processes in bone tissue.

DMA has been utilized in characterization of cortical[52,53] and cancellous bone[54] (viscoelastic) mechanical properties and can detect changes in the mechanisms causing viscoelastic properties.[24,27,28,53,55] The frequency-scan methods as used in this study for measuring dynamic properties of bone might be particularly useful in the development of noninvasive tools for detecting the effect of damage in the tissue. Resonant frequency methods have been used for predicting mechanical properties of whole bones from various species.[56–58] Vibrational measurements have also been performed on humans *in vivo*.[59,60] A review of the application of vibrational methods in orthopaedics covers most of the work until 1999.[61] Although skepticism on the success of these methods in a clinical environment has been raised, primarily due to difficulties in dealing with soft tissues, encouraging results have also been reported. For instance, it has been demonstrated, using monkeys, that whole bone strength is predictable from *in vivo* vibrational analysis.[62] Furthermore, there is evolving technology that is promising for application of vibration-based methods to bone *in vivo*.[63] While it is not the purpose of this paper to outline these methodologies for *in vivo* use, the presence of such effort indicates that the basic science developed in this area will find clinical application in future.

In conclusion, loading cortical bone past the yield stress changes its viscoelastic properties. The change depends on the nature of the damage. Both low- and high-frequency energy dissipation mechanisms are changed. The increase in viscoelastic energy dissipation after mechanical damage for both low and high frequencies is proposed as a potential toughening mechanism for bone. Future experiments should be designed to specifically address this possibility.

References

1. Frost HM. Presence of microscopic cracks in vivo in bone. Henry Ford Hosp Med Bull 1960;8:25–35.
2. Schaffler MB, Choi K, Milgrom C. Aging and matrix microdamage accumulation in human compact bone. Bone 1995;17: 521–525.
3. Wenzel TE, Schaffler MB, Fyhrie DP. In vivo microcracks in human vertebral trabecular bone. Bone 1996;19:89–95.
4. Norman TL, Wang Z. Microdamage of human cortical bone: Incidence and morphology in long bones. Bone 1997;20:375–379.
5. Frost HM, Bone microdamage: Factors that impairs its repair. In: Uhthoff HK, editor. Current Concepts of Bone Fragility. Berlin: Springer-Verlag; 1986, pp 123–239.
6. Radin EL, Parker HG, Pugh JW, Steinberg RS, Paul IL, Rose RM. Response of joints to impact loading, Part 3. Relationship between trabecular microfractures and cartilage degeneration. J Biomech 1973;6:51–57.
7. Farkas T, Boyd RD, Schaffler MB, Radin EL, Burr DB. Early vascular changes in rabbit subchondral bone after repetitive impulsive loading. Clin Orthop 1987:259–267.
8. Muir P, Johnson KA, Ruaux-Mason CP. In vivo matrix microdamage in a naturally occurring canine fatigue fracture. Bone 1999;25:571–576.
9. Johnston CC Jr, Slemenda CW. Pathogenesis of osteoporosis. Bone 1995;17:19S–22S.
10. Burr DB, Forwood MR, Fyhrie DP, Martin RB, Schaffler MB, Turner CH. Bone microdamage and skeletal fragility in osteoporotic and stress fractures. J Bone Mineral Res 1997;12:6–15.
11. Heaney RP. The natural history of vertebral osteoporosis. Is low bone mass an epiphenomenon? Bone 1992;13 (Suppl 2): S23–S26.
12. Sherman S, Heaney RP, Parfitt AM, Hadley EC, Dutta C. NIA workshop on aging and bone quality, Bethesda, Sept 3–4, 1992. Calcif Tissue Int 1993;53:S1–S180.
13. Freeman MA, Todd RC, Pirie CJ. The role of fatigue in the pathogenesis of senile femoral neck fractures. J Bone Joint Surg Br B 1974;56:698–702.
14. Sokoloff L. The Biology of Degenarative Joint Disease. Chicago: University of Chicago Press; 1969.
15. Yeni YN, Fyhrie DP. Fatigue damage-fracture mechanics interaction in cortical bone. Bone 2002;30:509–514.
16. Zioupos P. Accumulation of in-vivo fatigue microdamage and its relation to biomechanical properties in ageing human cortical bone. J Microsc 2001;201:270–278.
17. Norman TL, Yeni YN, Brown CU, Wang Z. Influence of microdamage on fracture toughness of the human femur and tibia. Bone 1998;23:303–306.
18. Schaffler MB, Radin EL, Burr DB. Mechanical and morphological effects of strain rate on fatigue of compact bone. Bone 1989;10:207–214.
19. Schaffler MB, Radin EL, Burr DB. Long-term fatigue behavior of compact bone at low strain magnitude and rate. Bone 1990;11:321–326.
20. Carter DR, Hayes WC. Compact bone fatigue damage. I. Residual strength and stiffness. J Biomech 1977;10:325–337.

21. Chamay A. Mechanical and morphological aspects of experimental overload and fatigue in bone. J Biomech 1970;3:263–270.
22. Zioupos P, Casinos A. Cumulative damage and the response of human bone in two-step loading fatigue. J Biomech 1998;31: 825–833.
23. Sobelman OS, Gibeling JC, Stover SM, Hazelwood SJ, Yeh OC, Shelton DR, Martin RB. Do microcracks decrease or increase fatigue resistance in cortical bone? J Biomech 2004;37:1295–1303.
24. Yeni YN, Christopherson GT, Turner AS, Les CM, Fyhrie DP. Apparent viscoelastic anisotropy as measured from nondestructive oscillatory tests can reflect the presence of a flaw in cortical bone. J Biomed Mater Res A 2004;69:124–130.
25. Menard KP. Dynamic mechanical analysis: A practical introduction. Boca Raton: CRC Press; 1999.
26. Gustafson MB, Martin RB, Gibson V, Storms DH, Stover SM, Gibeling J, Griffin L. Calcium buffering is required to maintain bone stiffness in saline solution. J Biomech 1996;29:1191–1194.
27. Yeni YN, Kim DG, Dong XN, Turner AS, Les CM, Fyhrie DP. Do sacrificial bonds affect the viscoelastic and fracture properties of bone? Clin Orthop Relat Res 2006;443:101–108.
28. Les CM, Vance JL, Christopherson GT, Turner AS, Divine GW, Fyhrie DP. Long-term ovariectomy decreases ovine compact bone viscoelasticity. J Orthop Res 2005;23:869–876.
29. Gere JM, Timoshenko ST. Mechanics of Materials, 3rd ed. Boston: PWS-Kent Publishing Company; 1990.
30. Boyce TM, Fyhrie DP, Glotkowski MC, Radin EL, Schaffler MB. Damage type and strain mode associations in human compact bone bending fatigue. J Orthop Res 1998;16:322–329.
31. Lakes RS. Viscoelastic measurement techniques. Rev Sci Instrum. 2004;75:797–810.
32. Burr DB, Turner CH, Naick P, Forwood MR, Ambrosius W, Hasan MS, Pidaparti R. Does microdamage accumulation affect the mechanical properties of bone? J Biomech 1998;31:337–345.
33. Vashishth D, Koontz J, Qiu SJ, Lundin-Cannon D, Yeni YN, Schaffler MB, Fyhrie DP. In vivo diffuse damage in human vertebral cancellous bone. Bone 2000;26:147–152.
34. Jepsen KJ, Davy DT, Krzypow DJ. The role of the lamellar interface during torsional yielding of human cortical bone. J Biomech 1999;32:303–310.
35. ASTM, D 790M-93. Standard test methods for flexural properties of unreinforced and reinforced plastics and electrical insulating materials [Metric], in: Annual book of ASTM Standards; 1993.
36. ASTM, Standard test method for plane-strain fracture toughness of metallic materials. West Conshohocken, PA: American Society for Testing and Materials; 1997.
37. Arthur Moore TL, Gibson LJ. Microdamage accumulation in bovine trabecular bone in uniaxial compression. J Biomech Eng 2002;124:63–71.
38. Murayama T. Dynamic Mechanical Analysis of Polymeric Material. Materials Science Monographs, Vol. 1. Amsterdam: Elsevier; 1978.
39. Vashishth D, Behiri JC, Bonfield W. Crack growth resistance in cortical bone: Concept of microcrack toughening. J Biomech 1997;30:763–769.
40. Malik CL, Stover SM, Martin RB, Gibeling JC. Equine cortical bone exhibits rising R-curve fracture mechanics. J Biomech 2003;36:191–198.
41. Nalla RK, Kruzic JJ, Kinney JH, Ritchie RO. Effect of aging on the toughness of human cortical bone: Evaluation by R-curves. Bone 2004;35:1240–1246.
42. Vashishth D, Tanner KE, Bonfield W. Experimental validation of a microcracking-based toughening mechanism for cortical bone. J Biomech 2003;36:121–124.
43. Fyhrie DP, Vashishth D. Bone stiffness predicts strength similarly for human vertebral cancellous bone in compression and for cortical bone in tension. Bone 2000;26:169–173.
44. Hoshaw SJ, Cody DD, Saad AM, Fyhrie DP. Decrease in canine proximal femoral ultimate strength and stiffness due to fatigue damage. J Biomech 1997;30:323–329.
45. Vashishth D, Tanner KE, Bonfield W. Contribution, development and morphology of microcracking in cortical bone during crack propagation. J Biomech 2000;33:1169–1174.
46. Braidotti P, Branca FP, Stagni L. Scanning electron microscopy of human cortical bone failure surfaces. J Biomech 1997; 30:155–162.
47. Pezzotti G, Sakakura S. Study of the toughening mechanisms in bone and biomimetic hydroxyapatite materials using Raman microprobe spectroscopy. J Biomed Mater Res A 2003;65:229–236.
48. Fantner GE, Hassenkam T, Kindt JH, Weaver JC, Birkedal H, Pechenik L, Cutroni JA, Cidade GA, Stucky GD, Morse DE, Hansma PK. Sacrificial bonds and hidden length dissipate energy as mineralized fibrils separate during bone fracture. Nat Mater 2005;4:612–616.
49. Thompson JB, Kindt JH, Drake B, Hansma HG, Morse DE, Hansma PK. Bone indentation recovery time correlates with bond reforming time. Nature 2001;414:773–776.
50. Currey J. Sacrificial bonds heal bone. Nature 2001;414:699.
51. Gao H, Ji B, Buehler MJ, Yao H. Flaw tolerant bulk and surface nanostructures of biological systems. Mech Chem Biosyst 2004;1:37–52.
52. Yamashita J, Furman BR, Rawls HR, Wang X, Agrawal CM. The use of dynamic mechanical analysis to assess the viscoelastic properties of human cortical bone. J Biomed Mater Res 2001;58:47–53.
53. Yamashita J, Li X, Furman BR, Rawls HR, Wang X, Agrawal CM. Collagen and bone viscoelasticity: A dynamic mechanical analysis. J Biomed Mater Res 2002;63:31–36.
54. Dong XN, Yeni YN, Les CM, Fyhrie DP. Effects of end boundary conditions and specimen geometry on the viscoelastic properties of cancellous bone measured by dynamic mechanical analysis. J Biomed Mater Res A 2004;68:573–583.
55. Les CM, Spence CA, Vance JL, Christopherson GT, Patel B, Turner AS, Divine GW, Fyhrie DP. Determinants of ovine compact bone viscoelastic properties: Effects of architecture, mineralization, and remodeling. Bone 2004;35:729–738.
56. Lowet G, Vanaudekercke R, Vanderperre G, Geusens P, Dequeker J, Lammens J. The relation between resonant frequencies and torsional stiffness of long bones in vitro—Validation of a simple beam model. J Biomech 1993;26:689–696.
57. Civitelli R, Abbasijarhomi SH, Halstead LR, Dimarogonas A. Ipriflavone improves bone-density and biomechanical properties of adult male-rat bones. Calcif Tissue Int 1995;56:215–219.
58. Civitelli R. In vitro and in vivo effects of ipriflavone on bone formation and bone biomechanics. Calcif Tissue Int 1997;61: S12–S14.
59. McCabe F, Zhou LJ, Steele CR, Marcus R. Noninvasive assessment of ulnar bending stiffness in women. J Bone Mineral Res 1991;6:53–59.
60. VanderPerre G, Lowet G. In vivo assessment of bone mechanical properties by vibration and ultrasonic wave propagation analysis. Bone 1996;18:S29–S35.
61. Nokes LDM. The use of low-frequency vibration measurement in orthopaedics. Proceedings of the Institution of Mechanical Engineers Part H. J Eng Med 1999;213:271–290.
62. Roberts SG, Hutchinson TM, Arnaud SB, Kiratli BJ, Martin RB, Steele CR. Noninvasive determination of bone mechanical properties using vibration response: A refined model and validation in vivo. J Biomech 1996;29:91–98.
63. Calle S, Remenieras JP, Matar OB, Defontaine M, Patat F. Application of nonlinear phenomena induced by focused ultrasound to bone imaging. Ultrasound Med Biol 2003;29: 465–472.